AD

TECHNICAL REPORT ARCCB-TR-02002

GUN BARREL VIBRATION ABSORBER TO INCREASE ACCURACY

ANDREW LITTLEFIELD
ERIC KATHE
ROBERT MESSIER
KENNETH OLSEN

FEBRUARY 2002

US ARMY ARMAMENT RESEARCH,
DEVELOPMENT AND ENGINEERING CENTER
CLOSE COMBAT ARMAMENTS CENTER
BENÉT LABORATORIES
WATERVLIET, N.Y. 12189-4050

DISCLAIMER

The findings in this report are not to be construed as an official Department of the Army position unless so designated by other authorized documents.

The use of trade name(s) and/or manufacturer(s) does not constitute an official endorsement or approval.

DESTRUCTION NOTICE

For classified documents, follow the procedures in DoD 5200.22-M, Industrial Security Manual, Section II-19, or DoD 5200.1-R, Information Security Program Regulation, Chapter IX.

For unclassified, limited documents, destroy by any method that will prevent disclosure of contents or reconstruction of the document.

For unclassified, unlimited documents, destroy when the report is no longer needed. Do not return it to the originator.

REPORT DOCUMENTATION PAGE

Form Approved
OMS No. 0704-0188

1. AGENCY USE ONLY (Leave blank)	2. REPORT DATE	3. REPORT TYPE AND DATES COVERED
	February 2002	Final

4. TITLE AND SUBTITLE

GUN BARREL VIBRATION ABSORBER
TO INCREASE ACCURACY

5. FUNDING NUMBERS

AMCMS No. 6226.24.H191.1

6. AUTHOR(S)

Andrew Littlefield, Eric Kathe, Robert Messier, and Kenneth Olsen

7. PERFORMING ORGANIZATION NAME(S) AND ADDRESS(ES)

U.S. Army ARDEC
Benet Laboratories, AMSTA-AR-CCB-O
Watervliet, NY 12189-4050

8. PERFORMING ORGANIZATION REPORT NUMBER

ARCCB-TR-02002

9. SPONSORING/MONITORING AGENCY NAME(S) AND ADDRESS(ES)

U.S. Army ARDEC
Close Combat Armaments Center
Picatinny Arsenal, NJ 07806-5000

10. SPONSORING/MONITORING AGENCY REPORT NUMBER

11. SUPPLEMENTARY NOTES

Presented at the 42nd AIAA/ASME/ASCE/AHS/ASC Structures, Structural Dynamics, and Materials Conference, Seattle, WA, 16-19 April 2001. Published in proceedings of the conference.

12a. DISTRIBUTION/AVAILABILITY STATEMENT

Approved for public release; distribution unlimited.

12b. DISTRIBUTION CODE

13. ABSTRACT (Maximum 200 words)

Gun barrel vibrations lead to dispersion in the shot patterns. Thus, reducing these vibrations should lead to increased accuracy. Since the muzzle is the anti-node for all vibration modes and its vibrations have the greatest effect on shot dispersion, it is the obvious location to attempt to dampen the vibrations. A model of the gun barrel was created in MATLAB® and verified by modal impact testing. Modal impact testing was done for the barrel alone and for three different muzzle brake vibration absorber configurations. Additionally, the gun was fired with and without the absorber to determine its performance. Significant reduction in shot dispersion was observed.

14. SUBJECT TERMS	15. NUMBER OF PAGES
Gun Barrel, Vibrations, Accuracy, Vibration Absorber, Firing Test, Dynamics	19
	16. PRICE CODE

17. SECURITY CLASSIFICATION OF REPORT	18. SECURITY CLASSIFICATION OF THIS PAGE	19. SECURITY CLASSIFICATION OF ABSTRACT	20. LIMITATION OF ABSTRACT
UNCLASSIFIED	UNCLASSIFIED	UNCLASSIFIED	UL

TABLE OF CONTENTS

TABLES

LIST OF ILLUSTRATIONS

INTRODUCTION

Vibration of the gun barrel in rapid-fire systems leads to dispersion in the shot patterns. The wider the dispersion, the more rounds required to affect the desired damage on the enemy. An intuitive way to reduce this shot dispersion is to reduce the vibrations of the barrel. The end of the barrel is the anti-node for all vibration modes and its vibrations have the greatest effect on shot dispersion, so it is the obvious location to attempt to dampen the vibrations. This work focuses on doing just that.

The system under study in this work is the 25-mm M242 Bushmaster chain gun. It is part of the M2A3 and M3A3 Bradley Fighting Vehicle Systems and is designed to engage and defeat armored vehicles as well as provide suppression fire. When engaging armored enemy assets, such as armored personnel carriers, accuracy is extremely important. The M242 fires five different rounds, M791, M792, M793, M910, and M919, although only the M793 training round was used in the tests.

A gun barrel vibration absorber has previously been designed (ref 1) and tested (ref 2) for use on the 120-mm XM291 tank gun (ref 3). This design had the absorber as part of the gun's thermal shroud. The present effort (ref 4) differs in its unique location, application to rapid-fire gun systems, and its possible dual use as part of a fuse-setting system.

The vibration absorber being considered is of the proof mass actuator type and is mounted onto the muzzle brake. This allows for the absorber to be easily mounted and removed with the muzzle brake, while still acting at the barrel location of greatest vibration activity. Addition of the absorber reshapes the frequency response by moving the resonant modes and zeros. This shifting effectively rejects the vibrational energy. Also, the motion of the absorber enhances the dissipation of this energy.

First, the barrel is modeled in MATLAB® using a finite element approach (ref 5). The Euler-Bernoulli finite element technique is used to generate second-order equations-of-motion of the barrel as a nonuniform beam. These are then converted to the first-order state space domain and transformed into the frequency domain. Predictions for the mode shapes and resonant frequencies are generated. After completing the model, it is verified by performing modal impact testing on the barrel. These results are then used to fine-tune the model.

Testing of the barrel with different vibration absorbers is then conducted. Three different versions are used, the differences being the number of rods connecting the mass to the barrel. By varying the number of connecting rods, the stiffness, and thus the frequency, of the vibration absorber can be tuned.

Finally, firing results for the barrel with and without a vibration absorber are presented. The eight-rod vibration absorber was used for these tests and was not tuned to one of the barrel's modes. Even with this less than perfectly tuned absorber, significant reductions in shot dispersion were achieved.

MATLAB® MODEL

A finite element model of the barrel minus the vibration absorber was created in MATLAB®. Euler-Bernoulli beam approximations and Hermite-cubic interpolation functions are used to form the mass and stiffness matrices for the undamped second-order equations-of-motion by approximating the barrel, a continuous nonuniform beam, as a series of discrete elements. Continuity of lateral displacement and slope are imposed at the element boundaries. When assembled, these elements closely approximate the dynamics of the barrel.

The geometry of the barrel is entered in 1-mm increments and any noncircular cross sections are smeared together to become circular. This smearing was done to the lugs near the breech end and to the rifling. The mass of the beam is calculated by adding the mass of each of these slices. The actual shape of the beam can be seen in Figure 1. The model's version of this can be seen in Figure 2.

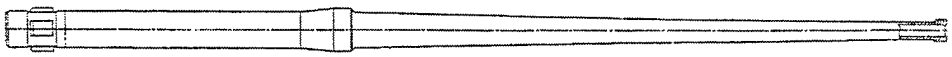

Figure 1. M242 barrel.

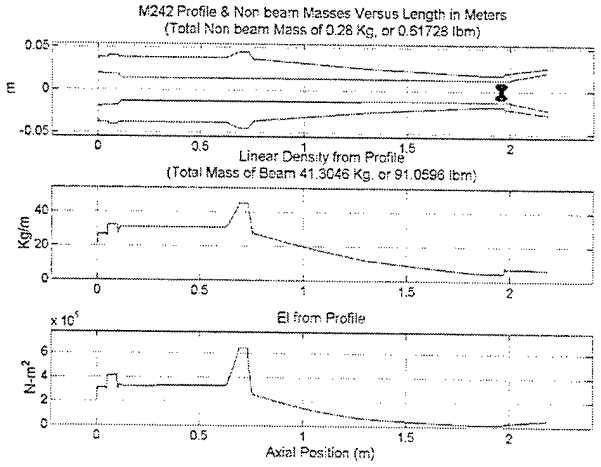

Figure 2. Barrel geometry.

The barrel actually ends just beyond the two-meter mark. The rest of the geometry is the muzzle brake. A Pro/Engineer model of the muzzle brake can be seen in Figure 3. The geometry is clearly too complicated to simply smear it together as was done with the rifling and lugs. Instead it was approximated as two hollow cylinders with different interior diameters followed by a hollow cone. The diameters of the cylinders and cones were selected so that both mass and location of the center of gravity of the approximate muzzle brake matched those of the Pro/Engineer model.

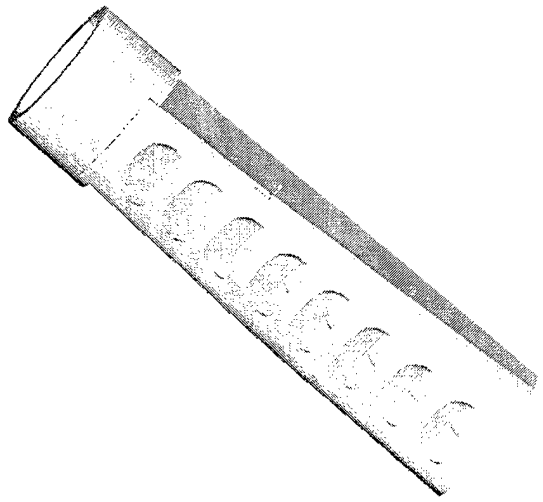

Figure 3. Pro/Engineer muzzle brake model.

After the geometry has been entered, the barrel is automatically broken into a user-defined number of elements. Nodes are forced to exist at both ends of the barrel and anyplace where constraints are specified. The springs used to hang the barrel during modal testing were entered as constraints in this fashion. The spring constant for the springs was found by hanging weights on them and measuring the deflection.

An additional node was specified at the same location as the response accelerometer. This accelerometer was located just rearward of the muzzle brake. This location should give a good indication of the muzzle's response. The mass of the accelerometer was also entered into the model and appears as the dark circles in Figure 2. The location of this specified node created small elements near the forward spring, so different numbers of elements were tried until they converged on a consistent value of the first natural frequency. The final number used was 36. Without this enforced node a smaller number of nodes may be used.

Rayleigh proportional damping is used in the model. The values entered were determined in a previous report using this software for analyzing an XM291 gun barrel (ref 1). After performing an experimental modal analysis on the barrel, experimentally found values were used and the model was rerun. Only minor differences in the resonant frequencies were found.

After the required data were entered, the model was run and output generated. The software generates undamped and damped mode shapes and natural frequencies, a pole-zero plot of the eigenvalues, time response of the muzzle to a breech impulse, and a bode plot of the muzzle response, plus additional plots about the quality of the finite element analysis (FEA). In this case we are interested in the damped mode shapes and natural frequencies. These can be found in Figure 4.

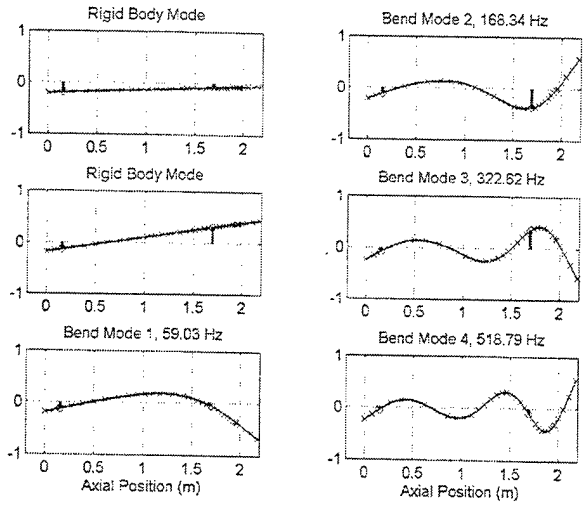

Figure 4. Damped mode shapes and natural frequencies.

MODAL IMPACT TESTING

After completion of the MATLAB® model, an experimental modal analysis was performed to validate the model. The barrel was hung from two springs to simulate a free-free condition. These springs were contained in the model as mentioned above. This did not present a perfect free-free situation but there is more than an order of magnitude between the highest rigid body mode (1.27 Hz) and the lowest flexible mode (59.03 Hz) so this was deemed satisfactory. Additionally the springs are explicitly represented in the model.

The goal of the modal analysis was to generate a frequency response plot between a force at the breech and the response of the muzzle. For this study an impact was used as the force and the acceleration of the muzzle was the response. An HP 3566A PC Spectrum/Network Analyzer was used to calculate the frequency response. A PCB Impact Hammer with a Delrin tip delivered the impact. The 6-dB roll-off point of the tip was found to be 1.605 kHz. A PCB ICP Accelerometer measured the response. The ICP power supply and signal conditioning for both of these was provided by a PCB 12-Channel Rack Mounted Power Unit with a variable gain of 0 to 100 per channel. This setup can be seen in Figure 5.

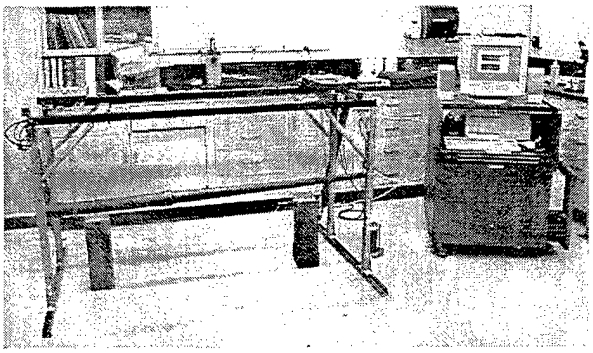

Figure 5. Experimental setup.

The HP 3566A was set up with a bandwidth of 800 Hz, 3200 frequency lines, and force/exponential windowing. Uniform averaging was performed with a total of 16 averages being used per run. The gain was set to provide good signal strength. After each impact the data were checked for double hits and overloading of the accelerometer.

The frequency response for barrel can be seen in Figure 6. The first four modes are plainly visible. A collocated pole-zero pair causes the strange behavior of the second mode. Examination of a pole-zero plot from MATLAB® shows this same behavior. Figure 7 shows this plot for the first four modes and how there is a zero collocated with the second mode.

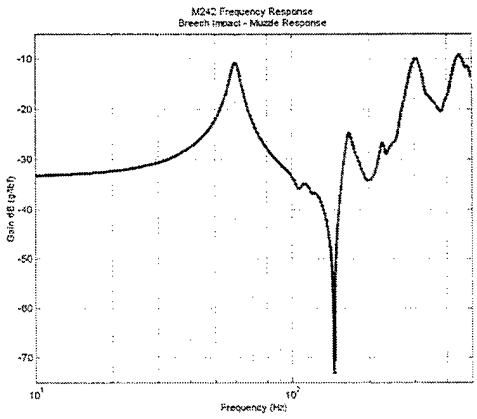

Figure 6. Plain barrel frequency response.

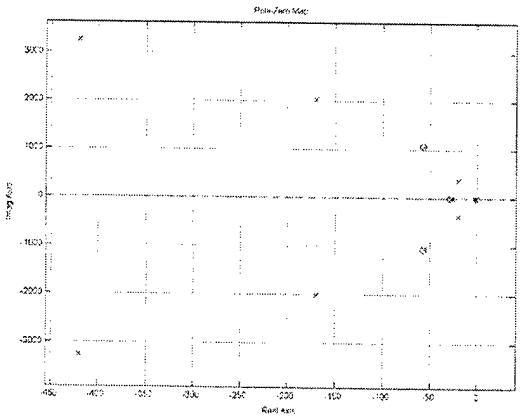

Figure 7. Pole-zero map for plain barrel.

The Peak Amplitude Method (ref 6) was used to extract the necessary modal parameters from the data. To determine the damping ratios, equations (1) and (2) were used.

$$\zeta = \frac{1}{2}\eta \tag{1}$$

$$\eta = \frac{1}{2}\frac{\omega_a^2 - \omega_b^2}{\omega_r^2} \tag{2}$$

where ξ is the viscous damping ratio, η is the structural damping loss factor, ω_r is the natural frequency of the peak, and ω_a and ω_b are the half-power points. These quantities can be seen in Figure 8.

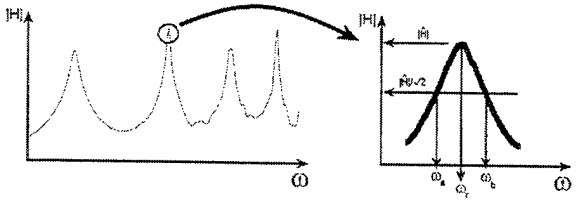

Figure 8. Peak Amplitude Method.

Once ξ has been found for at least two peaks, the proportional damping coefficients, α and β, can be found from the following formulas:

$$\alpha = -2\frac{\omega_1\omega_2(\omega_1\zeta_2\sqrt{1-\zeta_2^2} - \omega_2\zeta_1\sqrt{1-\zeta_1^2})}{-\omega_1^2 + \omega_1^2\zeta_2^2 - \omega_2^2\zeta_1^2 + \omega_2^2} \tag{3}$$

$$\beta = \frac{-\alpha + \alpha\zeta_2^2 + 2\zeta_2\sqrt{1-\zeta_2^2}\,\omega_2}{\omega_2^2} \tag{4}$$

Using these formulas, the following data in Table 1 were found for the data shown in Figure 6.

Table 1. Frequency Response Parameters from Modal Analysis

Plain Barrel with Muzzle Brake				
Peak	**Magnitude**	**Frequency**	**Coherence**	ζ
	dB (g/lb$_f$)	Hz		
1	-10.870	60.25	0.9990	0.0456
2	-24.710	167.25	0.9543	0.0361
3	-10.008	304.50	0.9306	
4	-9.117	448.25	0.9314	
α (s^{-1})		28.428		
β (s)		4.293E-05		

Comparison of these data with Figure 4 shows that the model predicted a stiffer system than was experimentally found. The higher in frequency one goes, the more divergent the model and reality become. We are concerned with low frequencies though, and the match between the model and experiment is very good for the first two modes. It is only off by about 1 Hz for these modes. This small amount of error is within what was seen from different runs and could be due to the accelerometer mounting and cabling and/or the nonideal connections of the support springs. The measured α and β were put back into the model to see if it would improve results, but no appreciable difference was found.

MATLAB® MODEL WITH VIBRATION ABSORBER

Now that the model has been validated for plain barrel, it must be modified to include the vibration absorber. The vibration absorber is a proof mass actuator that mounts to the muzzle brake. It consists of a 4.037-lb (1.831-kg) mass, suspended from spring rods that are attached to a collar, which is in turn press-fitted onto the standard muzzle brake. The rods are one-fourth inch (6.35-mm) in diameter and extend 5.8 inches (147.32-mm) from the collar to the mass.

There are three configurations of the vibration absorber: one with eight rods; another with four, the two middle ones removed top and bottom; and the last with two rods oriented diagonally. Only the eight- and four-rod versions were modeled, using the same number of nodes and enforced node locations as the plain barrel. The two-rod configuration was not modeled, as its boundary conditions do not allow it to be analyzed the same way as the other two. Since the vibration absorber mounts to the muzzle brake,

like before a Pro/Engineer model was used to ensure that mass and center of gravity location were correct for the entire assembly. Figure 9 shows the model.

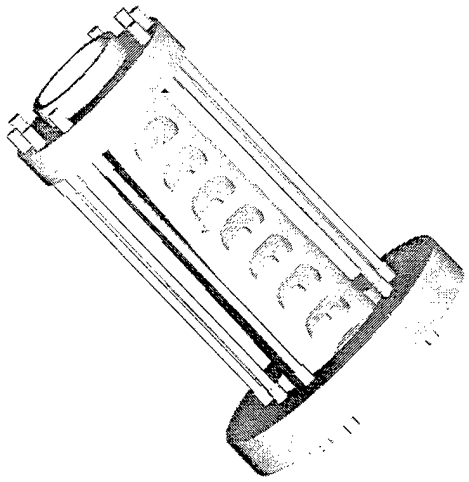

Figure 9. Pro/Engineer model of the vibration absorber.

The basic geometry of the muzzle brake was modified to include the retaining collar. This collar is made out of aluminum, but the MATLAB® model only has one density. So an equivalent geometry was created in steel to yield the same mass and center of gravity location. This was the only alteration made in the beam geometry.

The connecting rods were treated as springs, and thus by the standard approximation for a spring with mass, one-third of their mass was added to the absorber mass and two-thirds was added to the barrel as a lumped mass. The location of the lumped mass was adjusted so that the center of gravity of the rods and absorber mass together was positioned as in the actual assembly.

The MATLAB® model allows for a mass and stiffness to be entered for a vibration absorber. The mass was a combination of the absorber mass and one-third of the rod mass. The location for this mass was found by calculating the center of gravity for the combined absorber and one-third rod masses.

The stiffness of the absorber was found by performing a beam-bending test. Weights were hung off the end of the absorber and the displacement of the mass was measured. The rods were considered to act like cantilevered beams, with the collar end being rigidly fixed and the absorber end being allowed to displace vertically. This was then done for each configuration. The natural frequencies were found to be 41 and 29 Hz, respectively.

The geometry used by the model for the eight-rod absorber can be seen in Figure 10. The dark area near the muzzle brake is the mass of the accelerometer as before plus the distributed mass of one-third of the connecting rods. The only difference between the

eight-rod and four-rod versions of the model is the mass of the rods. For the four-rod version the nonbeam mass drops to 0.41947-kg.

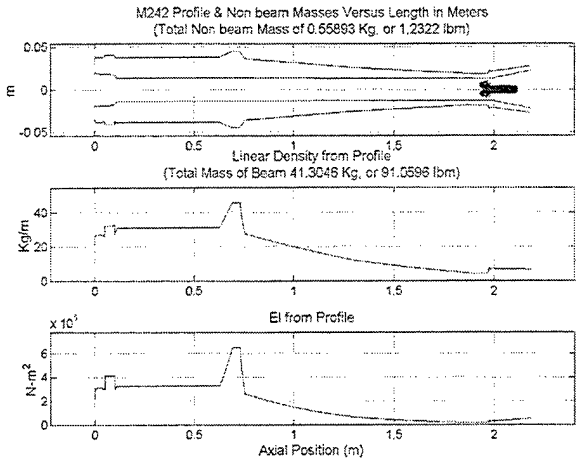

Figure 10. Barrel geometry with eight-rod vibration absorber.

As with the plain barrel, the models were run once all required data were entered. Damped mode shapes and natural frequencies were recovered along with bode plots and pole-zero maps. The damped mode shapes and natural frequencies can be seen in Figures 11 and 12. The circle at the end of the barrel represents the vibration absorber.

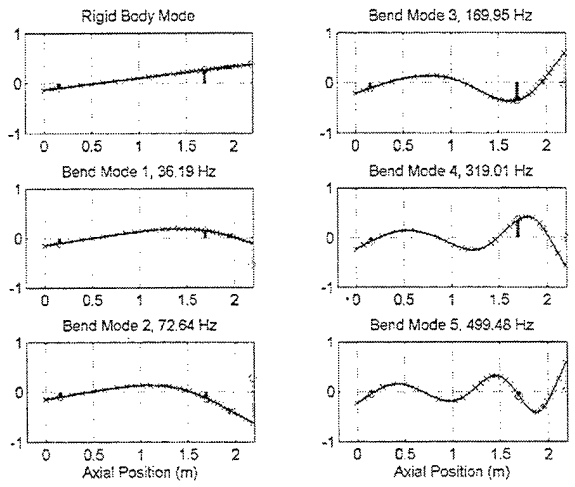

Figure 11. Damped mode shapes and natural frequencies for eight-rod absorber.

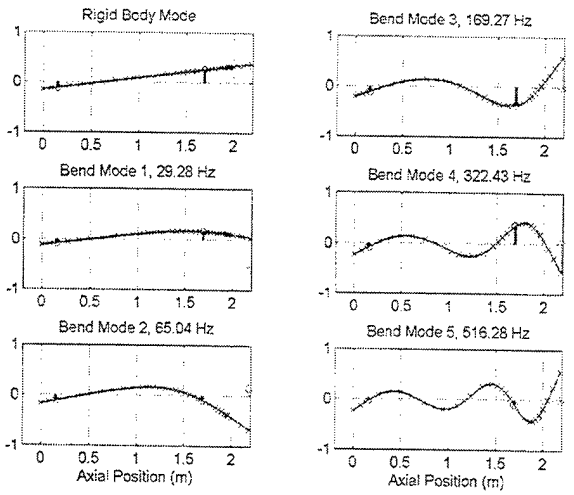

Figure 12. Damped mode shapes and natural frequencies for four-rod absorber.

VIBRATION ABSORBER TESTING

Now that we have a model including the vibration absorber, modal analyses were done on the different vibration absorber configurations. The barrel orientation and accelerometer placement were kept the same as the last plain barrel test. This ensured that any changes in the frequency response should be directly attributable to the vibration absorber and not changes in test setup.

Three configurations of the vibration absorber were tested: one with eight rods; another with four, the two middle ones removed top and bottom; and the last with two rods oriented diagonally. The four- and eight-rod versions were modeled in the previous section. The installed eight-rod absorber can be seen in Figure 13.

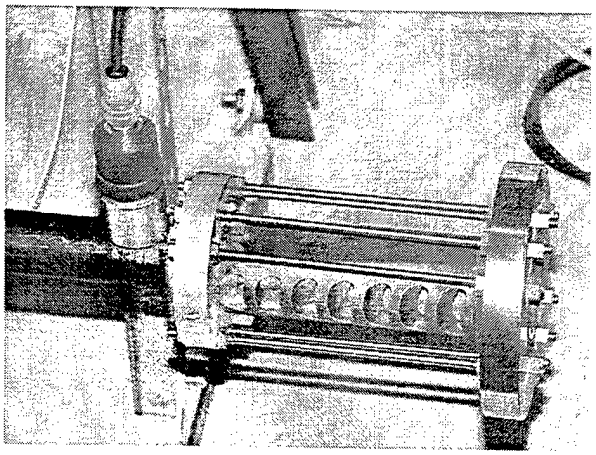

Figure 13. Installed vibration absorber.

The same testing procedure outlined above was used. The rods were removed with the absorber in place so as to minimize any test setup changes between the runs. The absorber was aligned such that the flats of the muzzle brake were parallel to the

floor. This is the normal firing position for the cannon. The results of the testing can be seen in Figure 14.

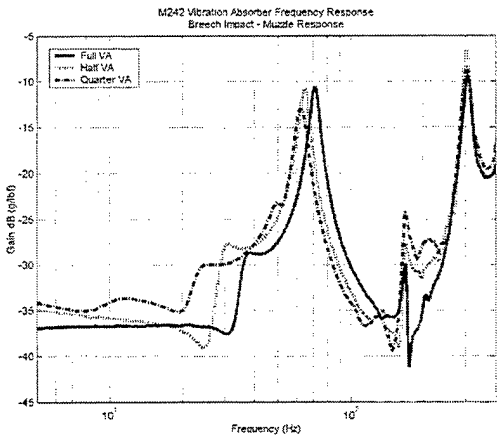

Figure 14. Vibration absorber frequency response.

A couple of points are obvious from the plot. First, the major difference between the different configurations is the amount the first peak of the plain barrel is shifted. As fewer rods are installed in the absorber, and thus the absorber stiffness decreases, the first peak moves to progressively lower frequencies. Not only the amount of shift but also the magnitude of the first peak appears to vary with absorber stiffness. At first glance, it appears that the eight- and four-rod vibration absorbers have the same magnitude, with the two-rod having a lower magnitude. This will be discussed more when numbers are culled from the data. Lastly, the higher frequency peaks appear to have been largely unchanged.

If the absorber's frequency had coincided with the first peak exactly, the peak would have been removed and its energy shifted into the new peaks on either side of it (ref 7). However, we do not have this case so the absorber pushes the peak to a higher frequency. Had the absorber's frequency been above that of the barrel's first mode, then it would have pushed the peak to a lower frequency. The additional pole-zero added by the absorber can be seen in the small resonance before the first peak. As stated earlier, the strange response at the barrel's second mode is due to a collocated pole-zero pair.

In order to draw more detailed conclusions and to compare to the nonvibration absorber results, actual numbers must be removed from the results. The same Peak Amplitude Method was used to pull out these data. The results of this analysis can be seen below in Table 2. The peaks are numbered to coincide with the ones in Table 1, with peak 0 being the absorber's own peak.

Table 2. Frequency Response Parameters from Vibration Absorber Testing

Full Vibration Absorber			
Peak	**Magnitude**	**Frequency**	**Coherence**
	dB (g/lb_f)	Hz	
0	-28.642	38.50	0.9937
1	-10.614	71.25	0.9991
2	-29.886	168.50	0.9887
3	-9.323	307.00	0.9139
4	-9.513	456.25	0.8915
Half Vibration Absorber			
Peak	**Magnitude**	**Frequency**	**Coherence**
	dB (g/lb_f)	Hz	
0	-27.683	31.25	0.9998
1	-10.793	64.50	1.0000
2	-27.711	169.75	0.9863
3	-6.541	304.00	0.8724
4	-6.054	460.75	0.8821
Quarter Vibration Absorber			
Peak	**Magnitude**	**Frequency**	**Coherence**
	dB (g/lb_f)	Hz	
0	-29.940	25.50	0.9996
1	-13.033	62.50	0.9995
2	-24.251	169.50	0.9777
3	-8.395	304.75	0.8640
4	-6.412	458.50	0.8528

From these numbers, it is apparent that the less stiff (i.e., fewer rods) the vibration absorber is, the lower it shifts the first frequency of the barrel. For the higher frequency peaks, it appears that the differences seen are due to errors in the data. As far as magnitude goes, there appears to be some contradictory data. It appears that the half-absorber produces larger magnitude gains than the full, but that the quarter-absorber produces smaller ones. This could be due to the fact that the quarter-absorber no longer has the same cantilever boundary conditions as the other two.

Comparison of these data with Figures 11 and 12 shows that the model overall predicted a stiffer system than was experimentally found; although the mode of the vibration absorber itself was found to be higher than predicted. This may be due to the way its stiffness was found. The higher in frequency one goes, the more divergent the model and reality become. We are primarily concerned with low frequencies though, and the match between the model and experiment is very good for the first three modes. It is only off by about 1 Hz for these modes. This small amount of error is within what was

seen from different runs and could be due to the accelerometer mounting and cabling and/or the nonideal connections of the support springs.

COMPARISON

Now that we have looked at the barrel by itself and with a vibration absorber separately, it is time to compare the two directly. Figure 15 shows the frequency response of the plain barrel and the three vibration absorber configurations. Figure 16 shows a close-up view of the first mode of the barrel.

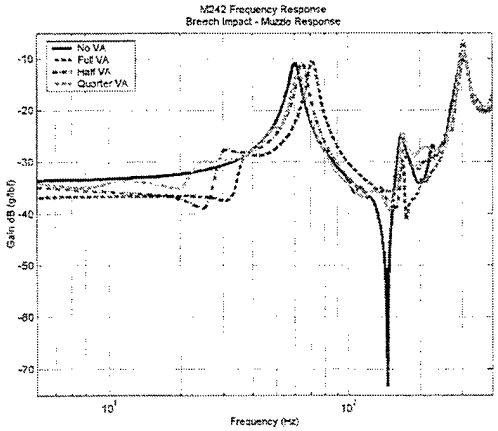

Figure 15. Frequency response comparison.

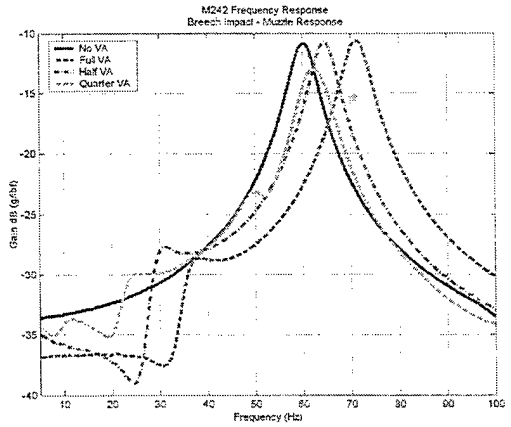

Figure 16. Frequency response comparison from 1 to 100 Hz.

Examining Figure 15, the two most obvious changes are the shifting of the first mode and the lessening of the zero around 150 Hz. The higher modes do not appear changed at all. Figure 16 shows the shifting of the first mode more clearly and how the two-rod version is able to reduce the magnitude of the first mode.

Comparing Tables 1and 2, one can see that these observations are borne out. The second and higher modes are hardly shifted, if at all, while the first one is shifted by as much as 11 Hz. This shifting is what allows the absorber to dampen the system's

vibrations. If the system resonance can be shifted away from the disturbance, then the vibrations will be reduced.

As stated previously, the inclusion of a vibration absorber shifts the modes around it away from its own mode. This accounts for the shifts seen in the barrel's first mode. As part of this shift, the absorber can also take energy from the peak it shifts. If the absorber's mode were coincident with one of the system resonances, then it would have split the mode and its energy into two smaller resonances.

The two-rod absorber is the only one that has an appreciable effect on the magnitude of the barrel's first mode. It reduces the magnitude by almost 3 dB. Due to its different boundary conditions though, this may not be as beneficial as it first seems. It could be that it is shifting energy from the vertical plane to the horizontal. Without further testing, it cannot be determined if this drop in the magnitude of the vertical response is beneficial or detrimental to system performance. An increase in horizontal motion would not be beneficial.

FIRING DATA

Laboratory experiments can tell us a lot, but does this change in frequency response translate into performance gains in the field? An M242 Bushmaster was fired at Benét's Gun Dynamics Laboratory with and without the eight-rod vibration absorber installed. Both single- and five-round bursts were fired for a total of 50 rounds. A picture of this firing can be seen in Figure 17.

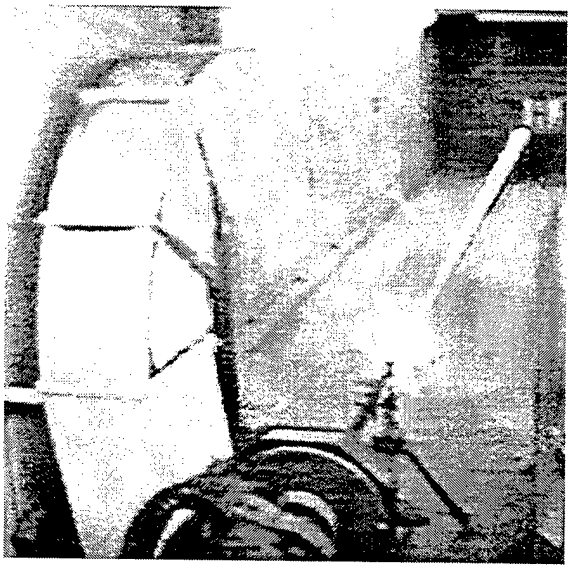

Figure 17. Firing the M242.

Figure 18 shows the muzzle vibrations (left) and orbits (right) during five-round burst fire. The muzzle vibrations clearly show that the absorber reduces the magnitude of the vertical vibrations. Up to a 45% attenuation of vertical motion was seen. A better appreciation for the effects of the absorber can be seen in the orbit plots. From here, it is obvious that the absorber reduced the barrel vibrations by about half. The increased tightness and repeatability of the trajectories bodes well for increased performance over the baseline system. However, the effect of this reduced vibration on accuracy was not possible due to the short projectile flight in the Gun Dynamics Laboratory (ref 8).

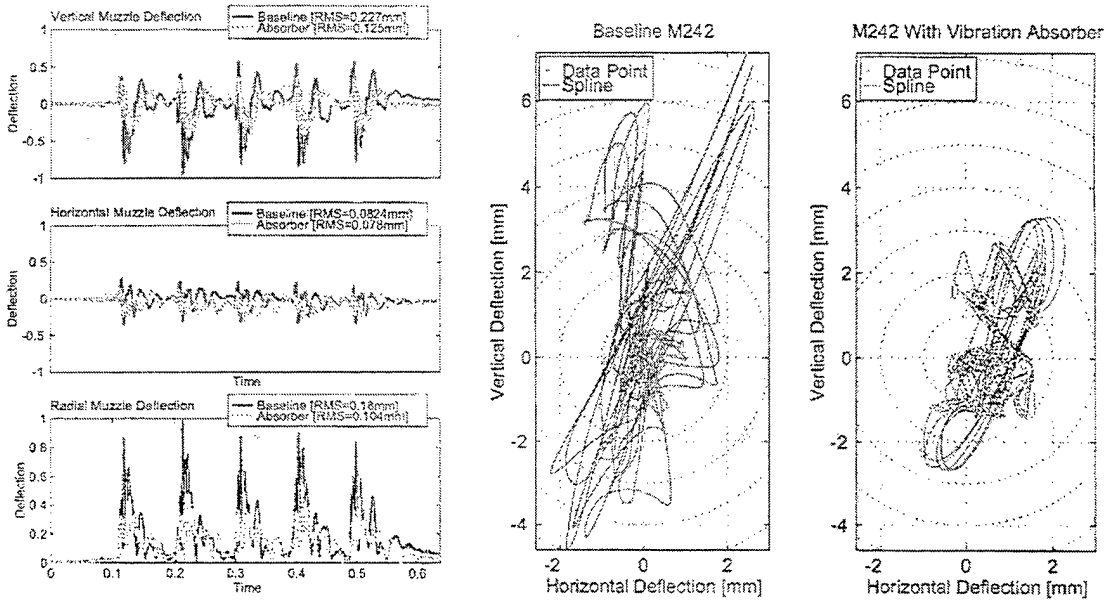

Figure 18. Firing results of the M242 with and without the vibration absorber.

This firing was done before the concept of a four- or two-rod absorber was developed, so no firing was done in those configurations. This may be pursued in later testing.

CONCLUSIONS

This report has shown the effect of mounting a vibration absorber to the muzzle brake of an M242 Bushmaster. A MATLAB® model of the barrel was developed and then verified by performing modal impact testing upon the actual barrel. Good agreement was found between the model and experimental data.

After modeling and testing the plain barrel, a vibration absorber was modeled and tested to find its effects upon the barrel's frequency response. Two different configurations were modeled, while three were tested. As with the plain barrel, good agreement was found between the model and reality. It was found that the absorber

shifted the first resonant frequency of the barrel higher in frequency, and that the two-rod version of the absorber reduced the magnitude of the response by 3 dB.

Finally, some firing data were presented to show the effectiveness of the absorber. The absorber was shown to decrease barrel vibrations by about half.

Overall, it was shown that by mounting a proof mass type actuator on the muzzle brake, the performance of the gun system could be increased. Since this is a part of the barrel designed to be screwed on and off, this allows for very easy mounting without affecting the rest of the gun system.

An additional advantage of mounting the absorber to the muzzle is that its mass ring may be combined with a muzzle fuse set device (ref 9). Previously a drawback of such devices was that they increased the weight affixed to the muzzle brake. Combining it with the absorber allows for its additional mass to be used to improve the gun's accuracy.

REFERENCES

1. Kathe, E., "Design and Validation of a Gun Barrel Vibration Absorber," *Proceedings of the 67th Shock and Vibration Symposium: Volume 1*, Monterey, CA, 18-22 November 1996, Published by SAVIAC, pp. 447-456.

2. Kathe E., "A Gun Barrel Vibration Absorber for Weapon Platforms Subject to Environmental Vibrations," *AIAA Paper No. 98-1846, A Collection of Technical Papers – 39th AIAA/ASME/ASCHE/AHS/ASC Structures, Structural Dynamics, and Materials Conference and Exhibit and AIAA/ASME/AHS Adaptive Structures Forum*, 1998, pp. 1284-1294.

3. Kathe, E., "Gun Barrel Vibration Absorber," U.S. Patent 6167794, January 2001.

4. Kathe, E., "Muzzle Brake Vibration Absorber," U.S. Patent Application Serial Number 09/898.376, filed 5 July 2001.

5. Kathe, E., "MATLAB® Modeling of Non-Uniform Beams Using the Finite Element Method for Dynamic Design and Analysis," ARDEC Technical Report ARCCB-TR-96010, Benet Laboratories, Watervliet, NY, April 1996.

6. Ewins, D.J., *Modal Testing: Theory, Practice, and Application*, Research Studies Press. Ltd., Baldock, England, 2000.

7. den Hartog, J.P., *Mechanical Vibrations*, McGraw-Hill Book Company, Inc., New York, 1956.

8. Kathe, E., "Lessons Learned on the Application of Vibration Absorbers for Enhanced Cannon Stabilization," *Proceedings of the Ninth U.S. Army Symposium on Gun Dynamics*, ARDEC Technical Report ARCCB-SP-99015 (E. Kathe, Ed.), Benet Laboratories, Watervliet, NY, November 1998, pp. 10.1-15.

9. Freymond, P.H., and Buckley, A., "Programmable Fuzing for Tube Launched Ammunition," *NDIA 35th Annual Gun and Ammunition Symposium*, Williamsburg, VA, May 2000.

TECHNICAL REPORT INTERNAL DISTRIBUTION LIST

	NO. OF COPIES
TECHNICAL LIBRARY ATTN: AMSTA-AR-CCB-O	5
TECHNICAL PUBLICATIONS & EDITING SECTION ATTN: AMSTA-AR-CCB-O	3
OPERATIONS DIRECTORATE ATTN: SIOWV-ODP-P	1
DIRECTOR, PROCUREMENT & CONTRACTING DIRECTORATE ATTN: SIOWV-PP	1
DIRECTOR, PRODUCT ASSURANCE & TEST DIRECTORATE ATTN: SIOWV-QA	1

NOTE: PLEASE NOTIFY DIRECTOR, BENÉT LABORATORIES, ATTN: AMSTA-AR-CCB-O OF ADDRESS CHANGES.

TECHNICAL REPORT EXTERNAL DISTRIBUTION LIST

	NO. OF COPIES
DEFENSE TECHNICAL INFO CENTER ATTN: DTIC-OCA (ACQUISITIONS) 8725 JOHN J. KINGMAN ROAD STE 0944 FT. BELVOIR, VA 22060-6218	2
COMMANDER U.S. ARMY ARDEC ATTN: AMSTA-AR-WEE, BLDG. 3022 AMSTA-AR-AET-O, BLDG. 183 AMSTA-AR-FSA, BLDG. 61 AMSTA-AR-FSX AMSTA-AR-FSA-M, BLDG. 61 SO AMSTA-AR-WEL-TL, BLDG. 59 PICATINNY ARSENAL, NJ 07806-5000	1 1 1 1 1 2
DIRECTOR U.S. ARMY RESEARCH LABORATORY ATTN: AMSRL-DD-T, BLDG. 305 ABERDEEN PROVING GROUND, MD 21005-5066	1
DIRECTOR U.S. ARMY RESEARCH LABORATORY ATTN: AMSRL-WM-MB (DR. B. BURNS) ABERDEEN PROVING GROUND, MD 21005-5066	1
COMMANDER U.S. ARMY RESEARCH OFFICE ATTN: TECHNICAL LIBRARIAN P.O. BOX 12211 4300 S. MIAMI BOULEVARD RESEARCH TRIANGLE PARK, NC 27709-2211	1

	NO. OF COPIES
COMMANDER ROCK ISLAND ARSENAL ATTN: SIORI-SEM-L ROCK ISLAND, IL 61299-5001	1
COMMANDER U.S. ARMY TANK-AUTMV R&D COMMAND ATTN: AMSTA-DDL (TECH LIBRARY) WARREN, MI 48397-5000	1
COMMANDER U.S. MILITARY ACADEMY ATTN: DEPT OF CIVIL & MECH ENGR WEST POINT, NY 10966-1792	1
U.S. ARMY AVIATION AND MISSILE COM REDSTONE SCIENTIFIC INFO CENTER ATTN: AMSAM-RD-OB-R (DOCUMENTS) REDSTONE ARSENAL, AL 35898-5000	2
COMMANDER U.S. ARMY FOREIGN SCI & TECH CENTER ATTN: DRXST-SD 220 7TH STREET, N.E. CHARLOTTESVILLE, VA 22901	1

NOTE: PLEASE NOTIFY COMMANDER, ARMAMENT RESEARCH, DEVELOPMENT, AND ENGINEERING CENTER, BENÉT LABORATORIES, CCAC, U.S. ARMY TANK-AUTOMOTIVE AND ARMAMENTS COMMAND, AMSTA-AR-CCB-O, WATERVLIET, NY 12189-4050 OF ADDRESS CHANGES.

DEPARTMENT OF THE ARMY
ARMAMENT RESEARCH, DEVELOPMENT AND ENGINEERING CENTER
BENÉT LABORATORIES, CCAC
US ARMY TANK-AUTOMOTIVE AND ARMAMENTS COMMAND
WATERVLIET, N.Y. 12189-4050

OFFICIAL BUSINESS
AMSTA-AR-CCB-O
TECHNICAL LIBRARY